Supporting information

A series of luminescence Cu(I) complexes based on diphosphine ligand and diimine ligand tuning by counter anions: the weak intermolecular interactions, terahertz spectra and photoproperties

Zi-Xi Li,[†a] Xiao-Nan Kuang,[†a] Guo Wang,[a] Ning Zhu,[a] Zhen-Zhou Sun,[a] Hong-Liang Han,[a] Yu-Ping Yang,[b] Zhong-Feng Li,[a] Xiu-Lan Xin,[c] Qiong-Hua Jin*[a,d], Zhi-Gang Ren*[e]

[a]*Department of Chemistry, Capital Normal University, Beijing 100048, China. E-mail: jinqh@cnu.edu.cn*
[b]*School of Science, Minzu University of China, Beijing 100081 China.*
[c]*School of Light Industry, Beijing Technology and Business University, Beijing 100048, China.*
[d]*State Key Laboratory of Structural Chemistry, Fujian Institute of Research on the Structure of Matter, Chinese Academy of Sciences, Fuzhou, Fujian 350002, China.*
[e]*College of Chemistry, Chemical Engineering and Materials Science, Soochow University, Suzhou 215123, China. E-mail: renzhigang@suda.edu.cn*
[†]***Zi-Xi Li*** *and* ***Xiao-Nan Kuang*** *contributed equally to this work.*
Electronic Supplementary Information (ESI) available: crystal structure information, spectra date and computation details. CCDC: 2103602, 1969929, 1969928, 2103705, 2103706.

Caption of Figure

Caption of Table

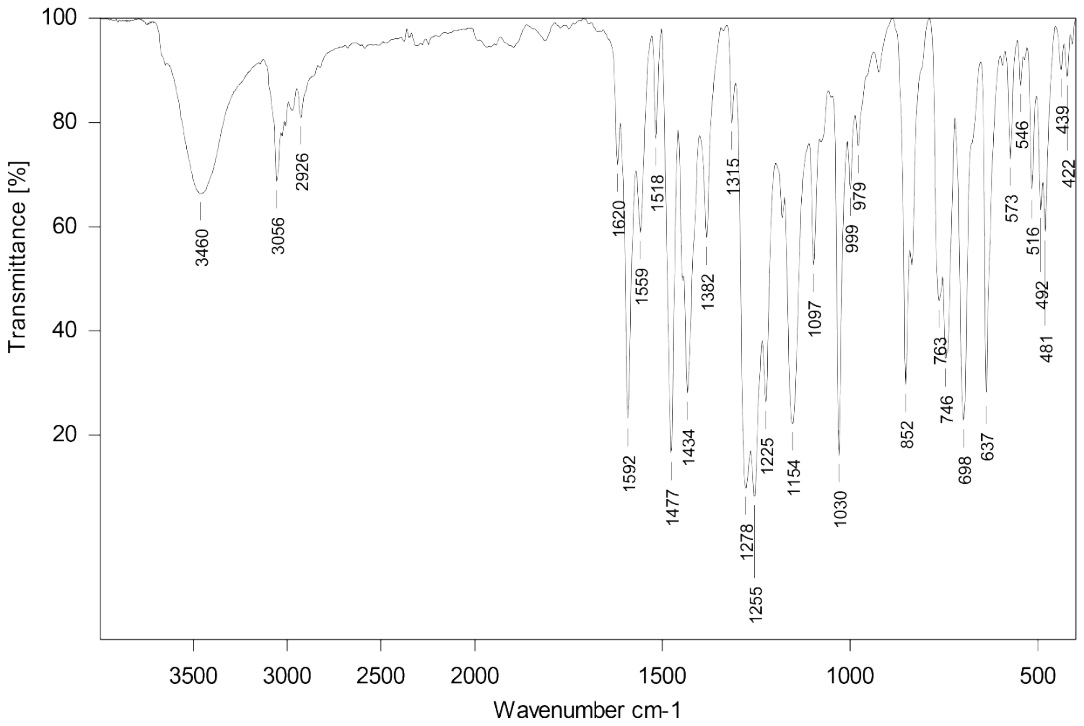

Fig. S1 The IR spectra for complex **1**.

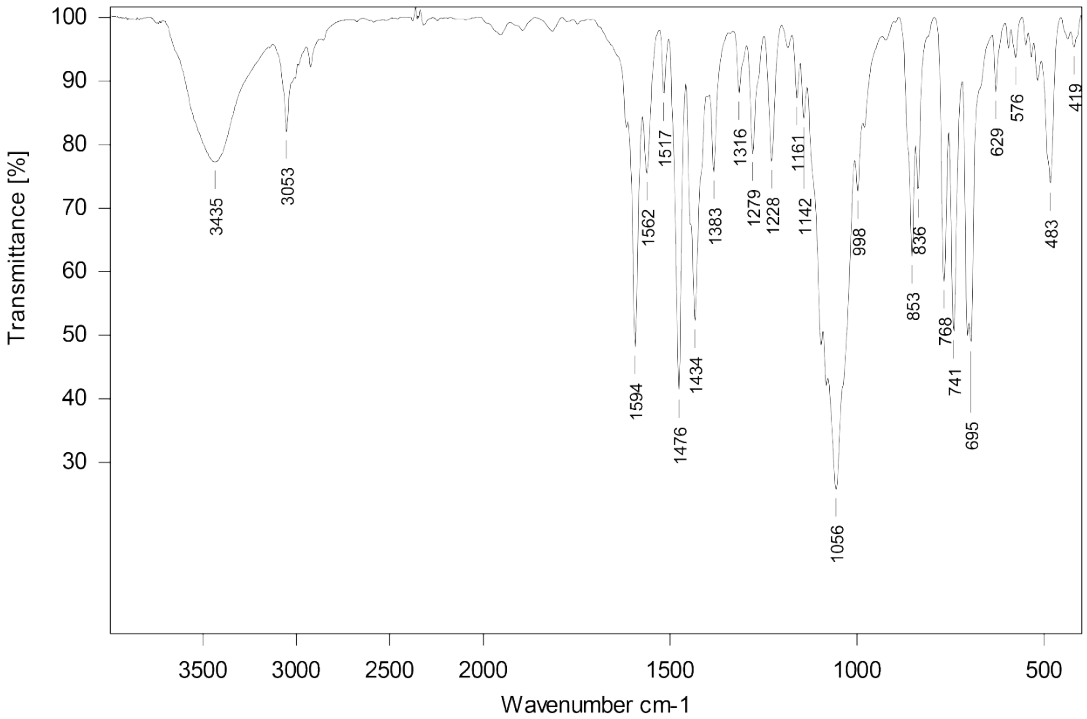

Fig. S2 The IR spectra for complex **2**.

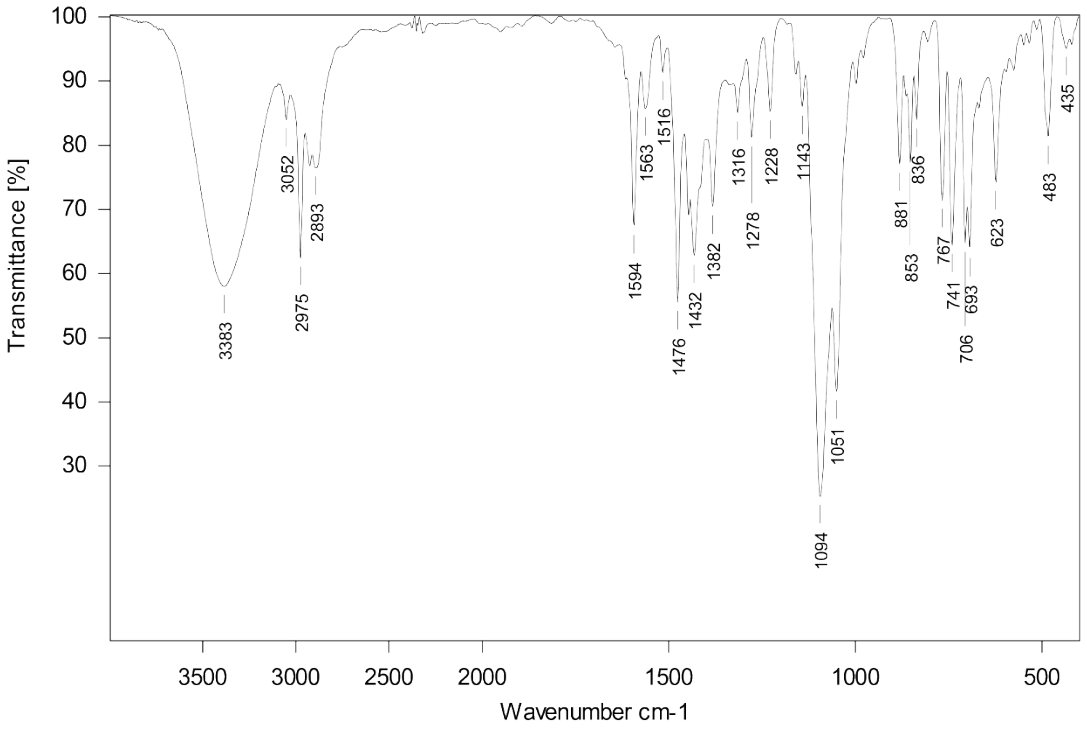

Fig. S3 The IR spectra for complex **3**.

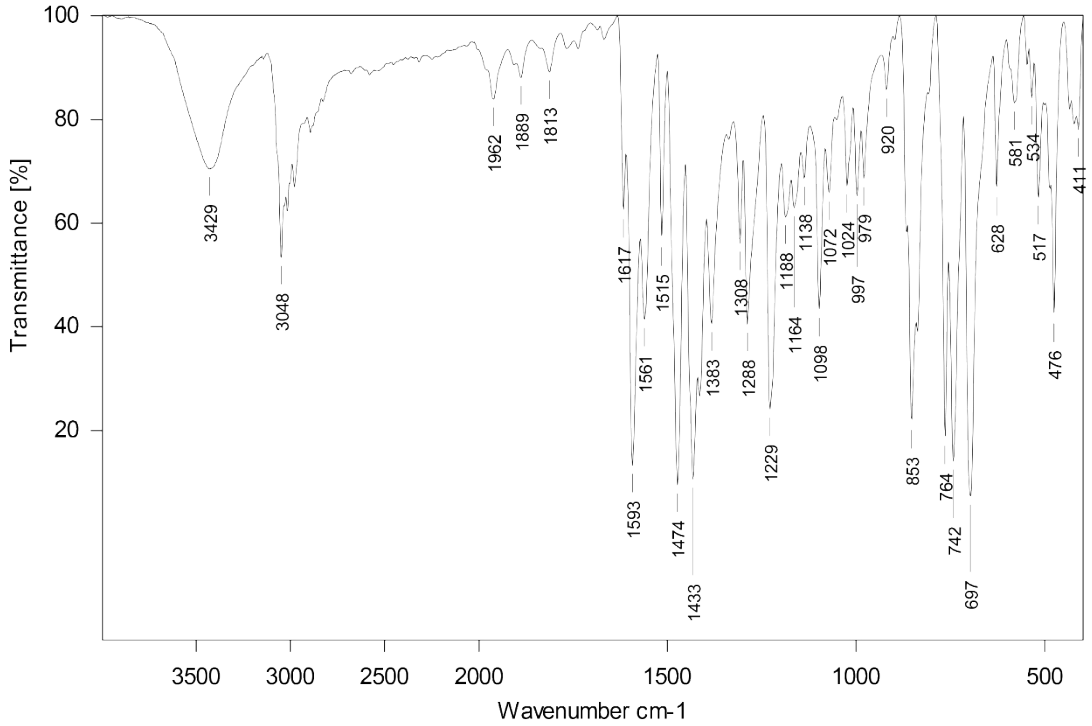

Fig. S4 The IR spectra for complex **4**.

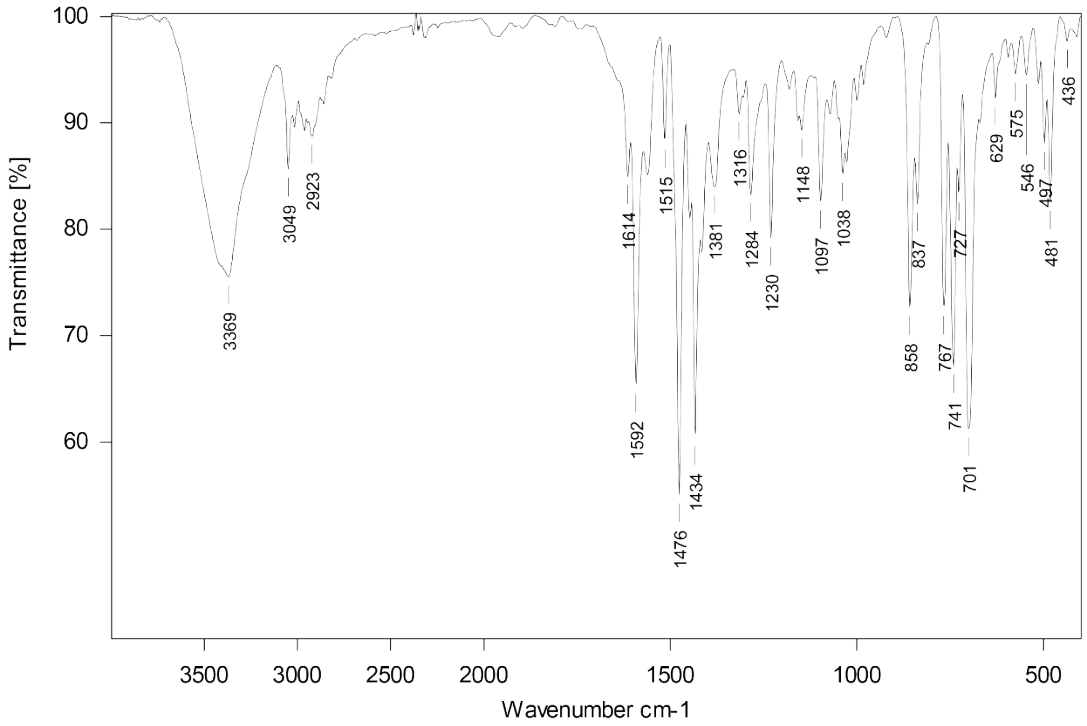

Fig. S5 The IR spectra for complex **5**.

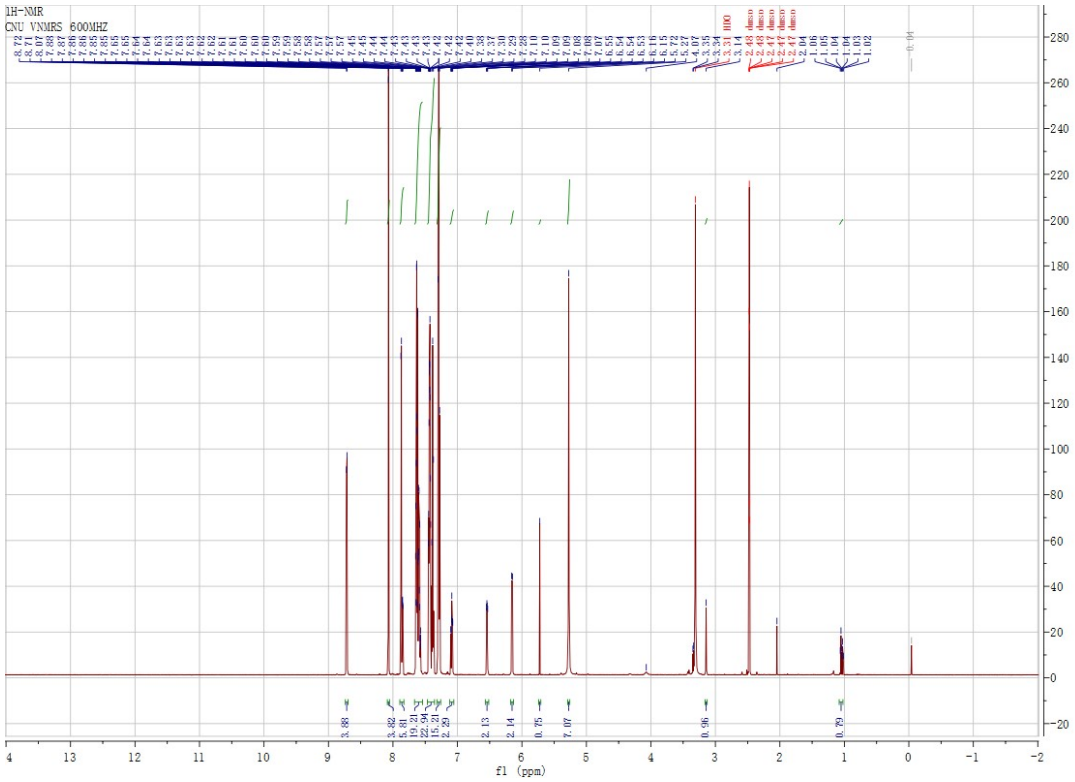

Fig. S6 The ^{1}H NMR spectra for complex **1**.

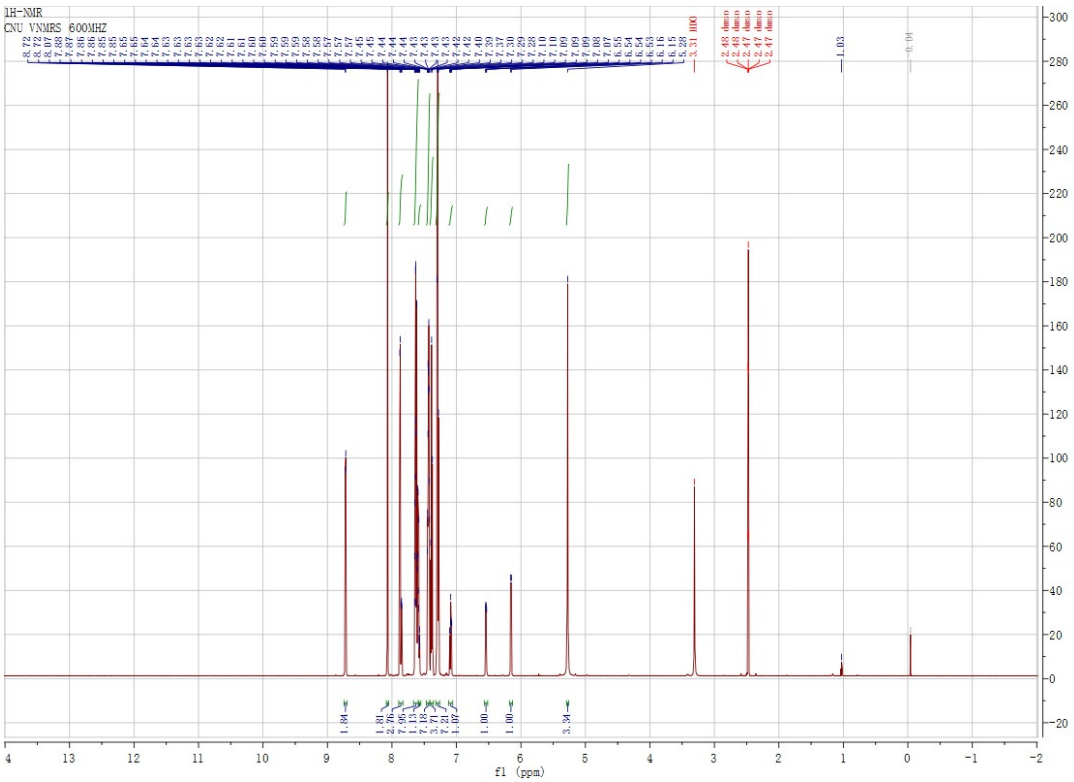

Fig. S7 The ^{1}H NMR spectra for complex **2**.

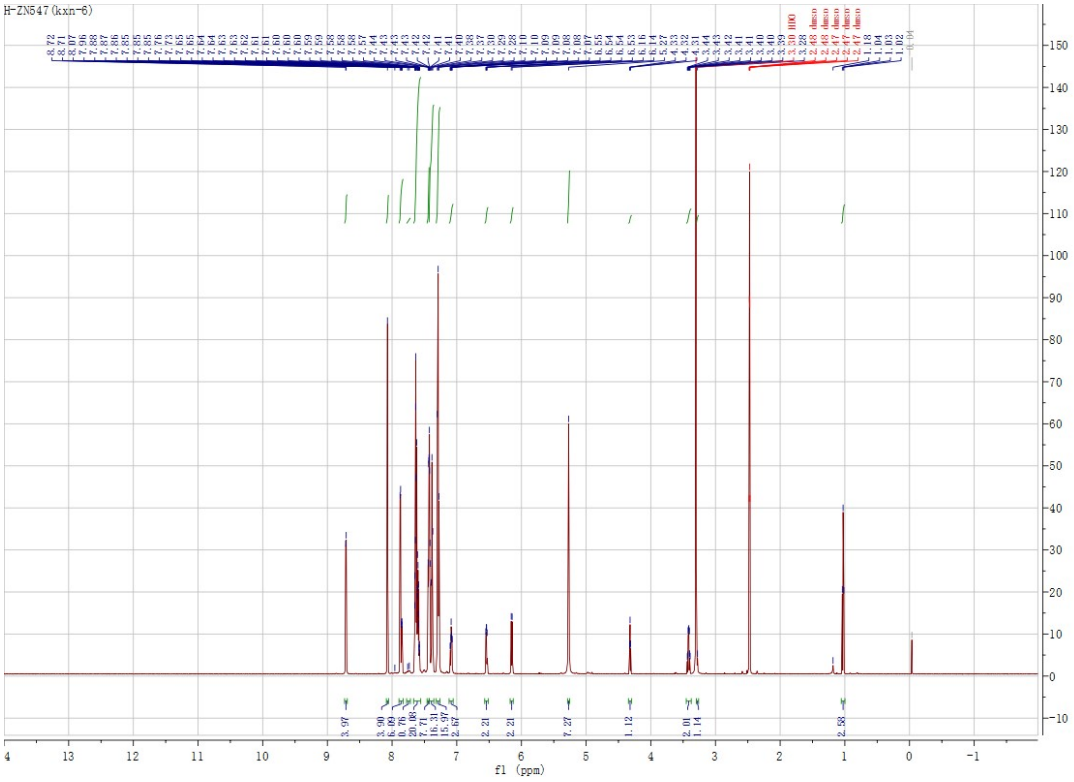

Fig. S8 The ^{1}H NMR spectra for complex **3**.

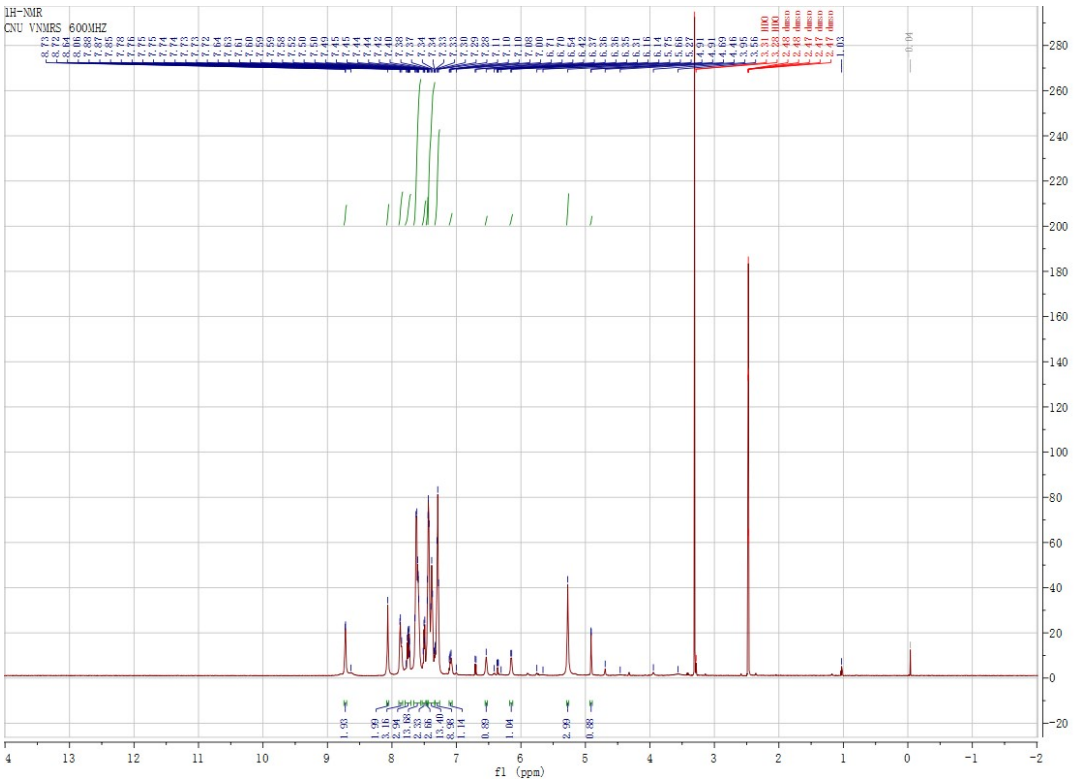

Fig. S9 The ^{1}H NMR spectra for complex **4**.

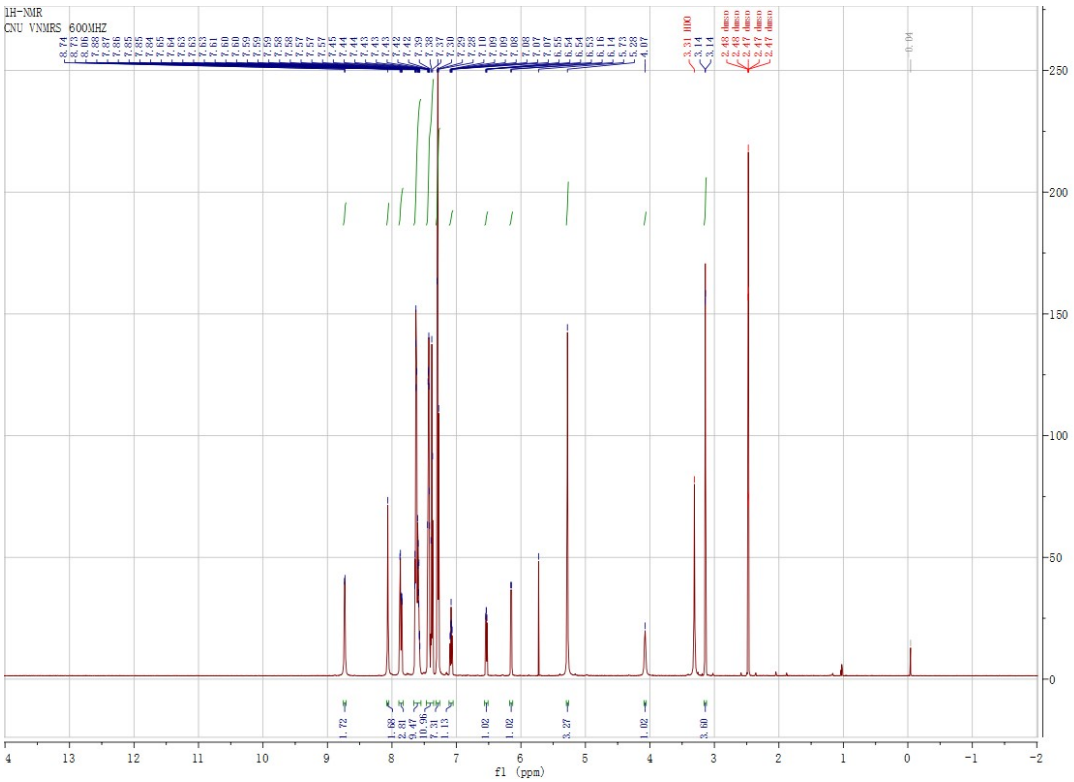

Fig. S10 The ^{1}H NMR spectra for complex **5**.

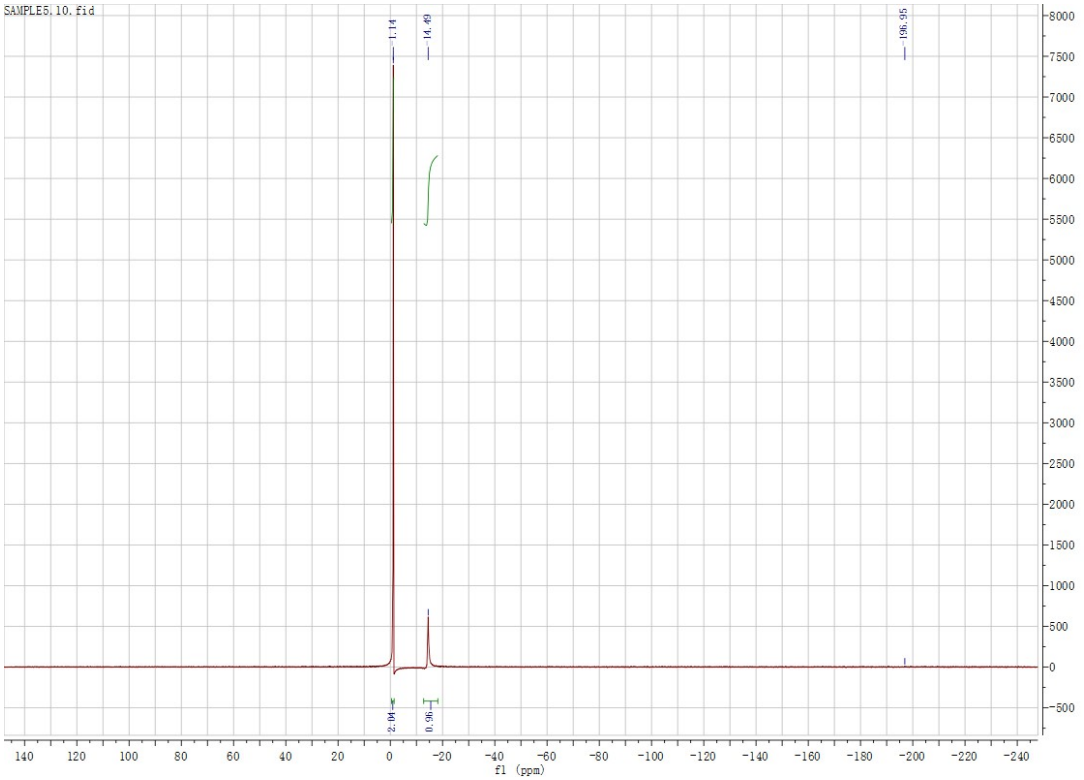

Fig. S11 The ^{31}P NMR spectra for complex **1**.

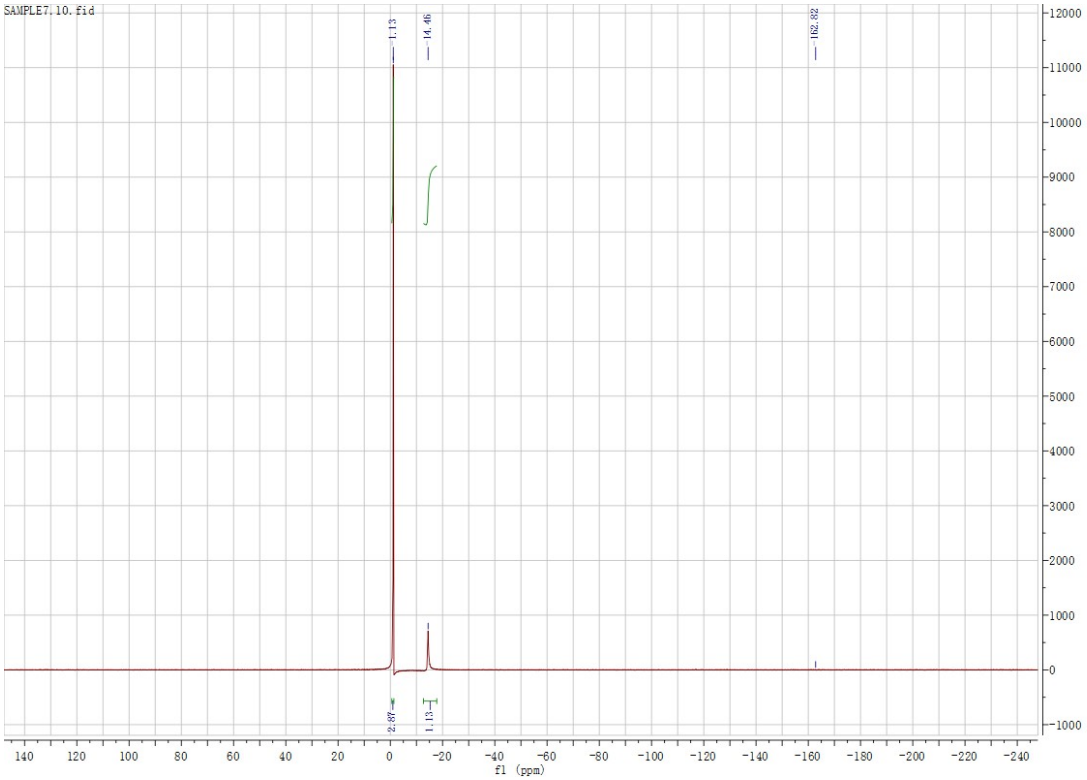

Fig. S12 The ^{31}P NMR spectra for complex **2**.

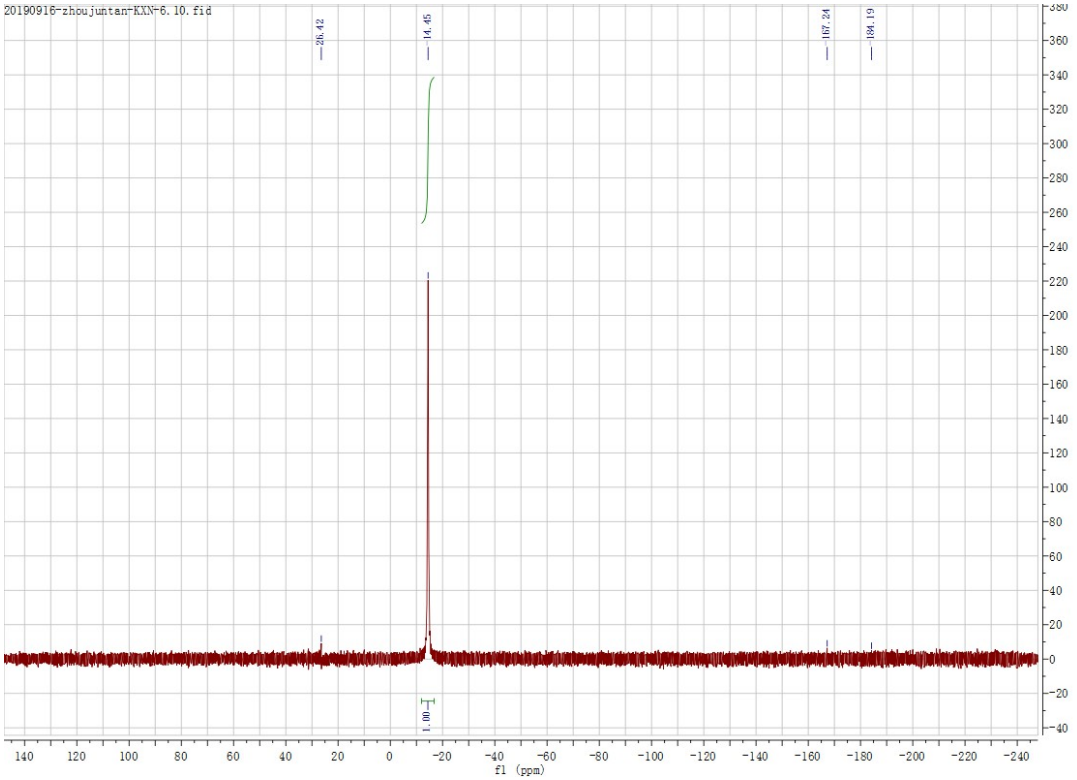

Fig. S13 The ^{31}P NMR spectra for complex **3**.

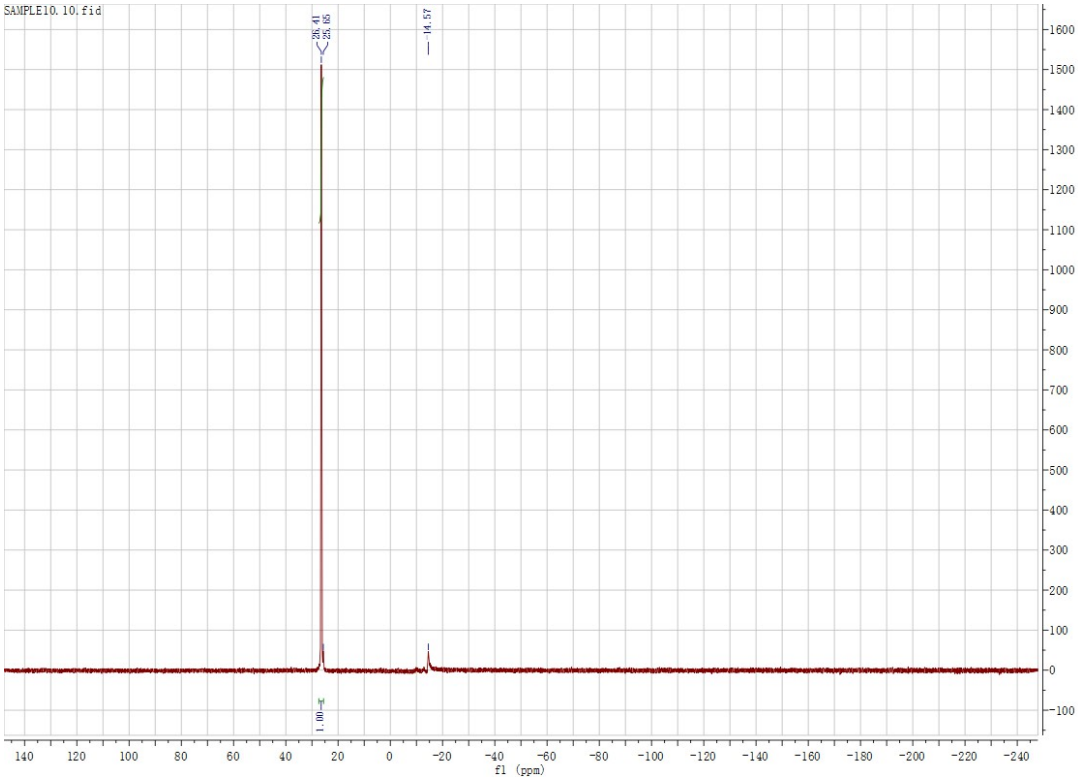

Fig. S14 The ^{31}P NMR spectra for complex **4**.

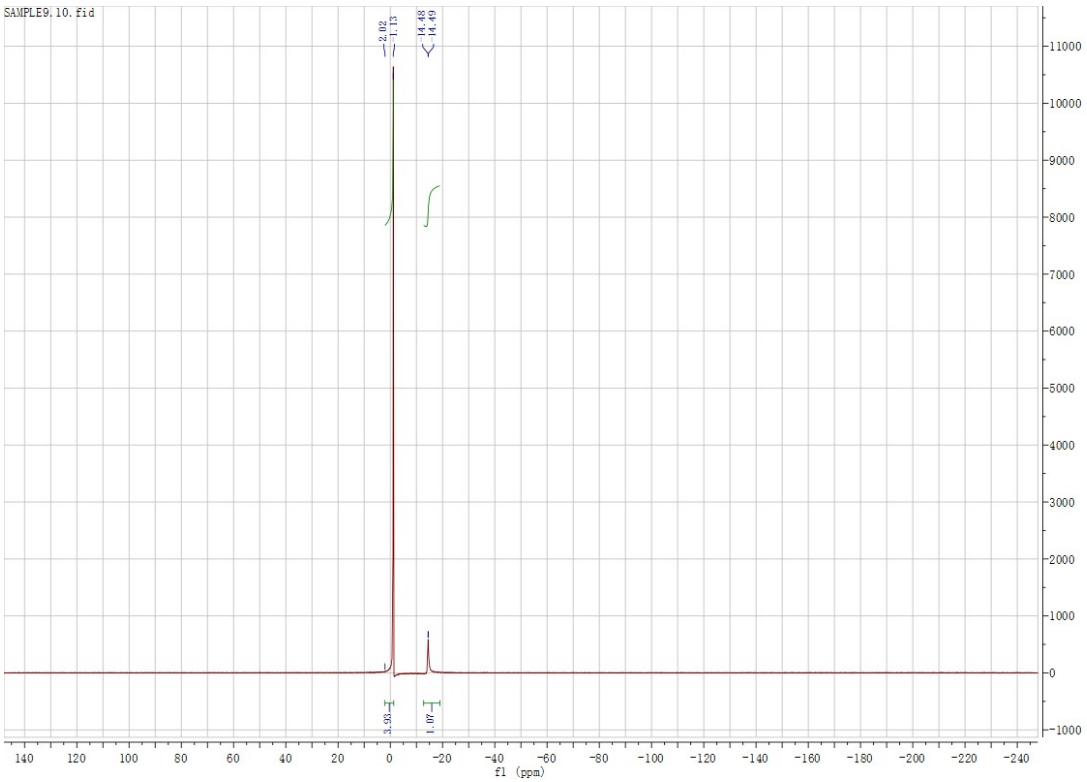

Fig. S15 The ^{31}P NMR spectra for complex **5**.

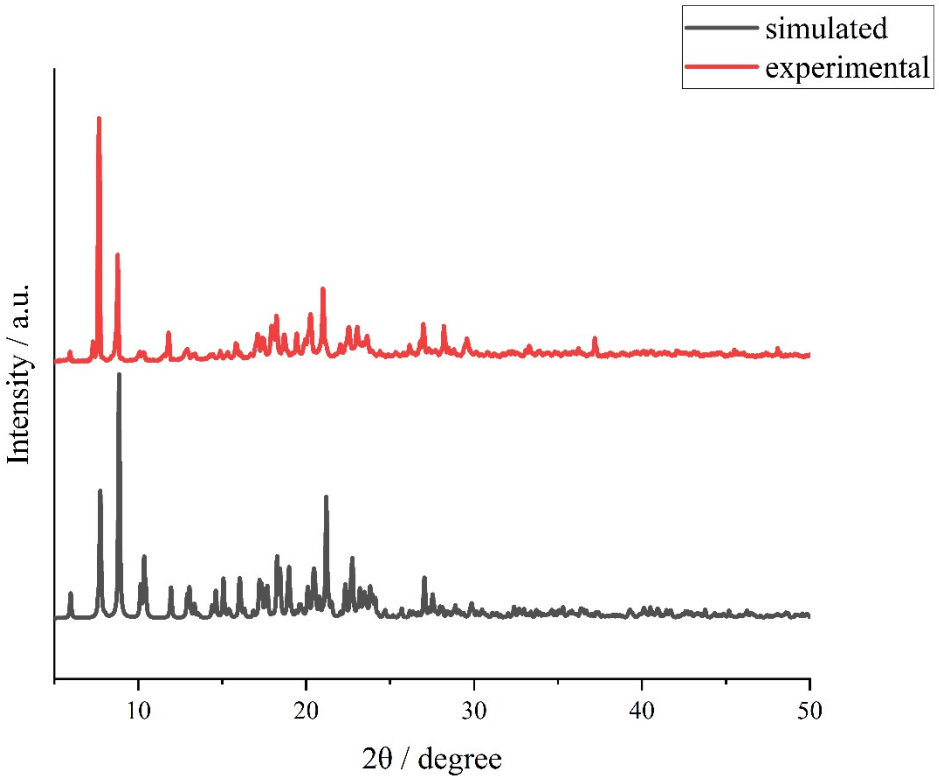

Fig. S16 The PXRD patterns for complex **1**: simulated from single crystal data (Black) and single phase polycrystalline sample (Red).

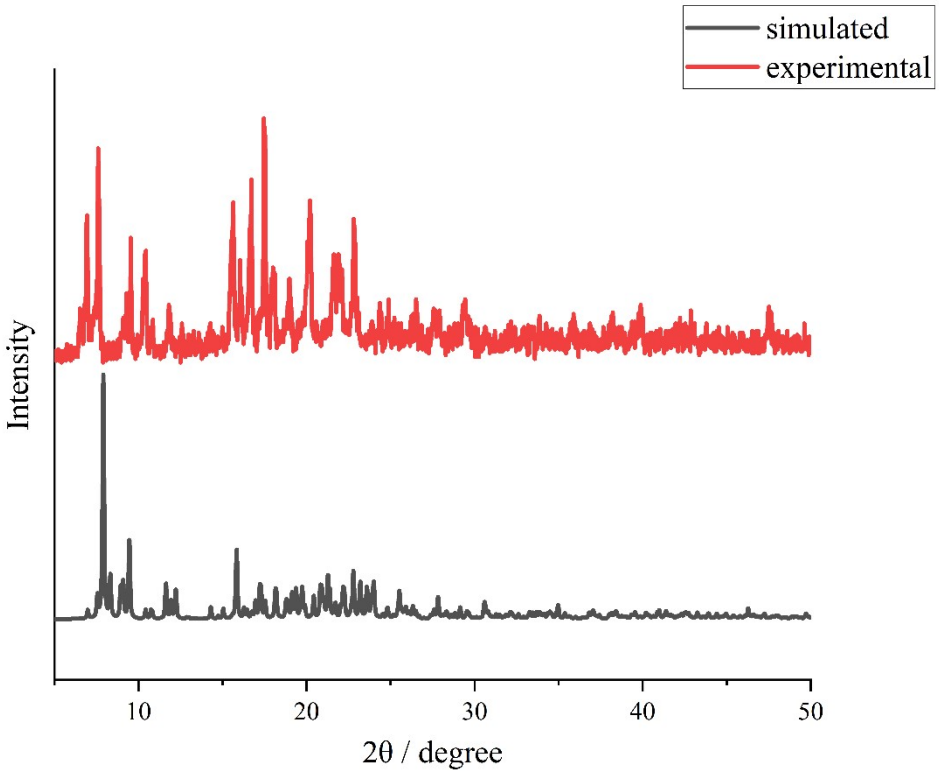

Fig. S17 The PXRD patterns for complex **2**: simulated from single crystal data (Black) and single phase polycrystalline sample (Red).

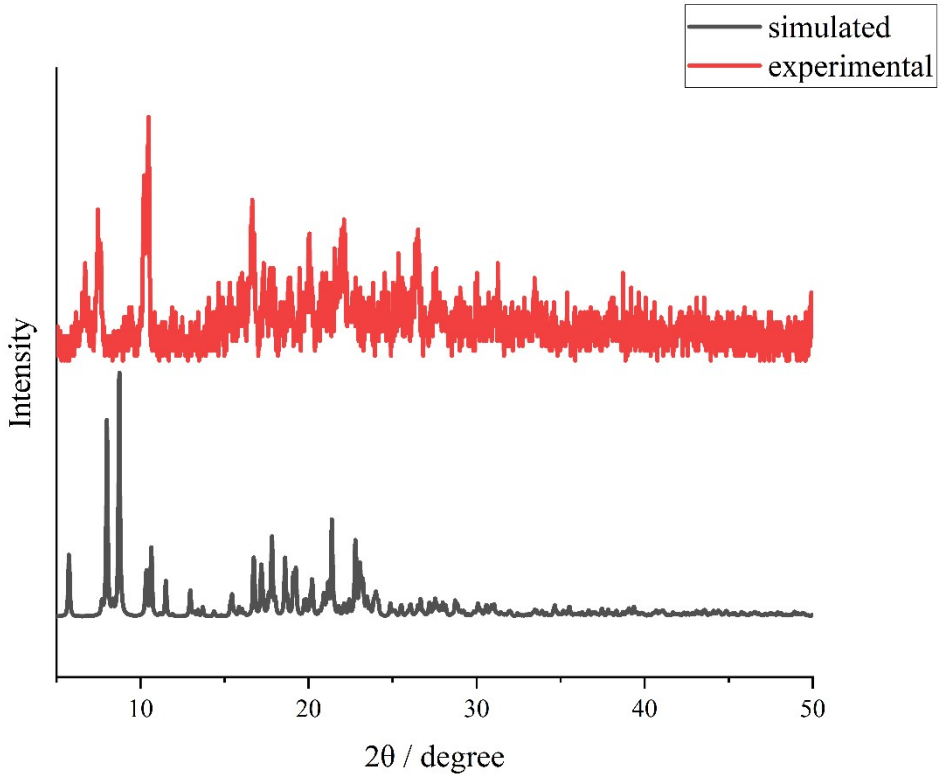

Fig. S18 The PXRD patterns for complex **3**: simulated from single crystal data (Black) and single phase polycrystalline sample (Red).

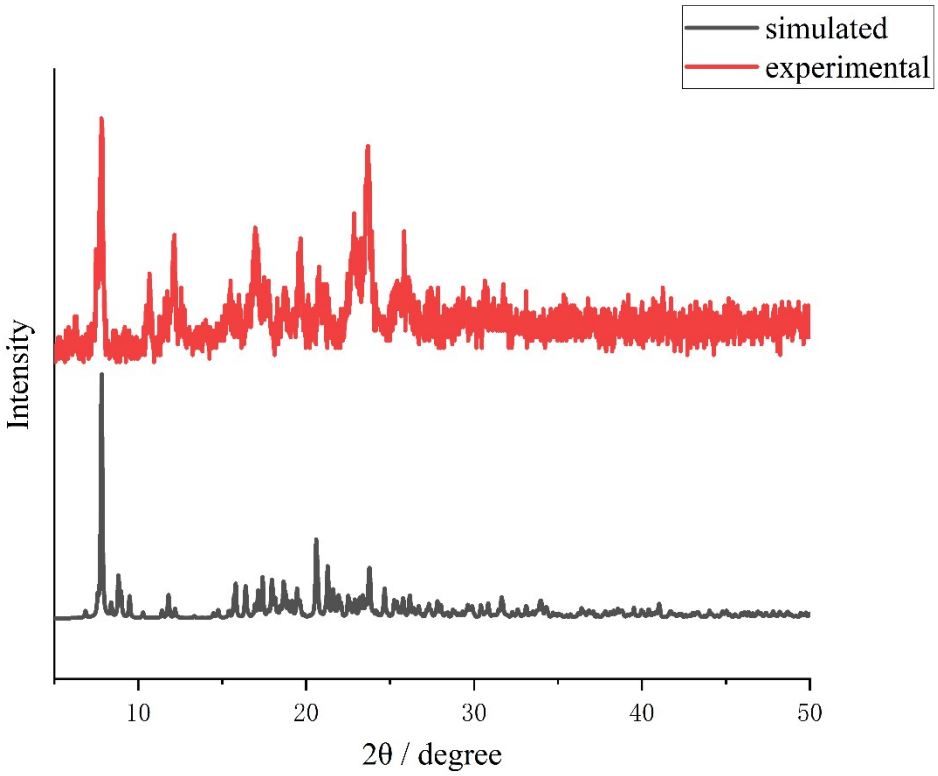

Fig. S19 The PXRD patterns for complex **4**: simulated from single crystal data (Black) and single phase polycrystalline sample (Red).

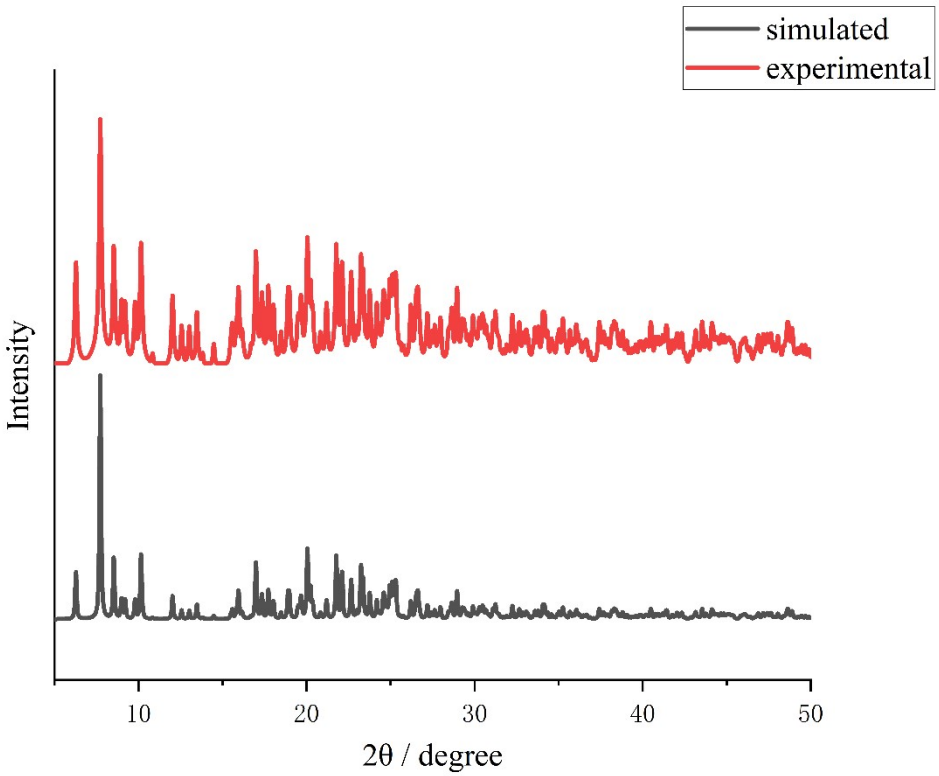

Fig. S20 The PXRD patterns for complex **5**: simulated from single crystal data (Black) and single phase polycrystalline sample (Red).

TGA was used to verify the stability of complexes **1-5** and the number of solvent molecules in the complexes (Fig. S21). As shown in graph, all the complexes presented weight loss related to the decomposition of ligands bdppmapy and Bphen. The TGA curves of complexes **2**, **4** and **5** all showed weight loss connected with the solvent moleculars in their crystal structures (**2**: 99.16% at 165 °C, cacld: 99.13%; **4**: 97.00% at 273 °C, cacld: 96.94%; **5**: 93.81% at 260 °C, cacld: 93.79%).

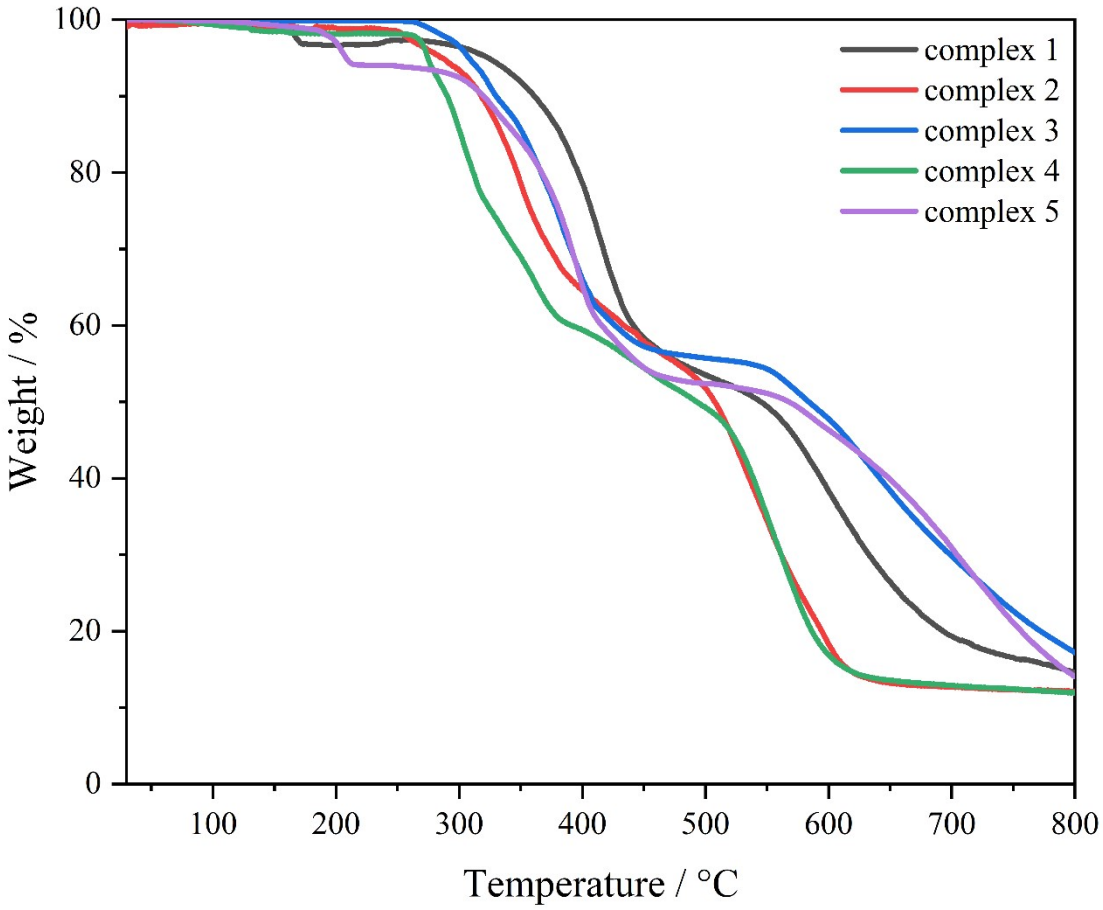

Fig. S21 The thermal stability curves for complexes **1-5**.

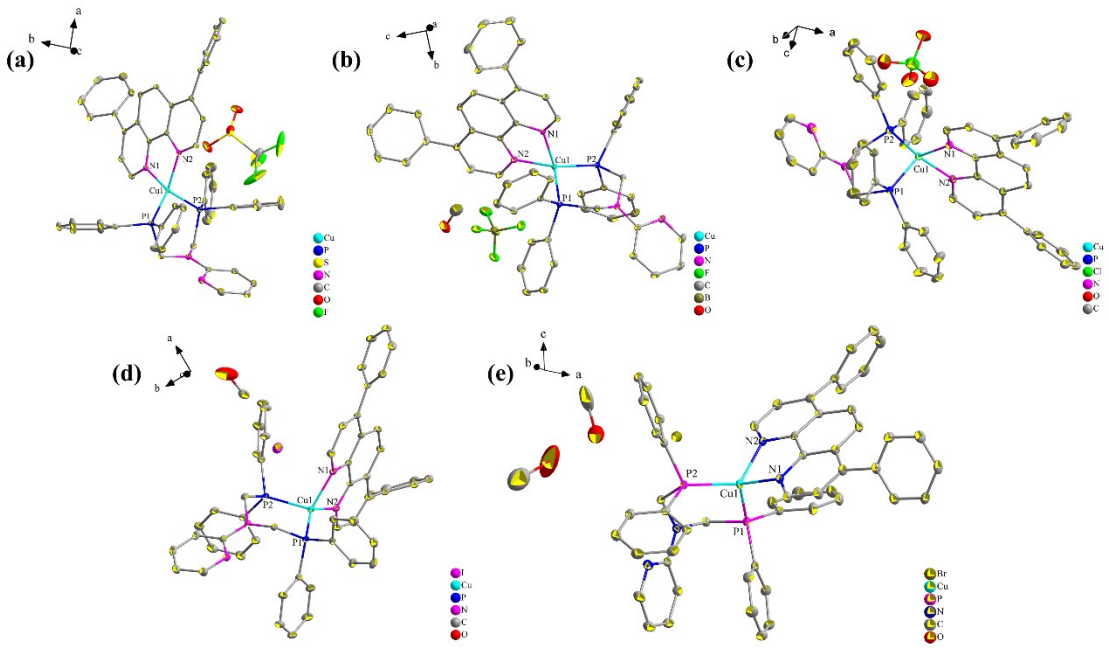

Fig. S22 Coordination environment of Cu(I) in complexes **1** (a), **2** (b), **3** (c), **4**(d), **5**(e) thermal ellipsoid drawn with a probability of 30%. For clarity, all hydrogen atoms and solvent molecules have been omitted.

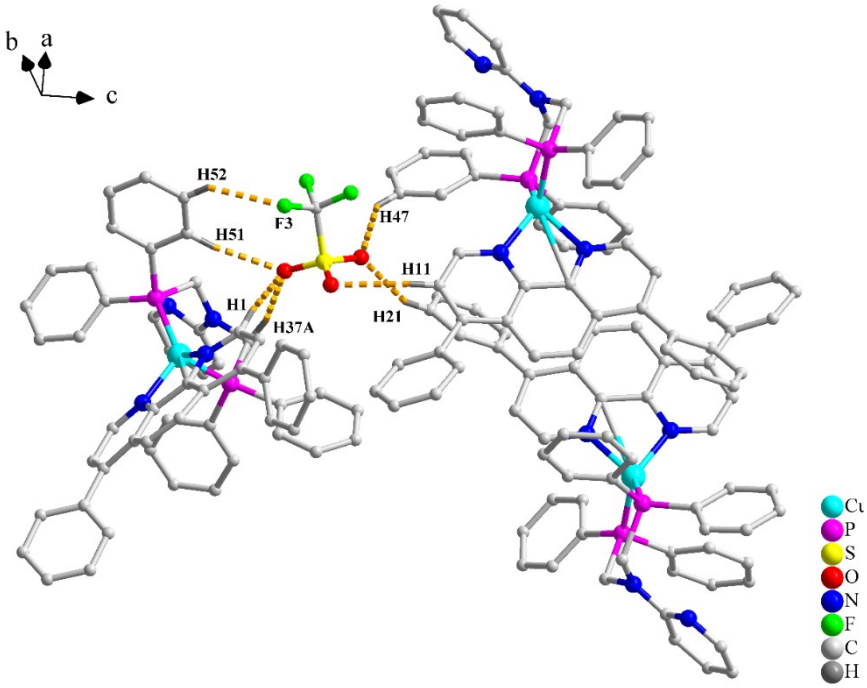

Fig. S23 Hydrogen bonds in **1** (C1-H1…O2, 2.49 Å; C11-H11…O1, 2.50 Å; C21-H21…O3, 2.34 Å; C37-H37A…O2, 2.47 Å; C47-H47…O3, 2.48 Å; C51-H51…O2, 2.44 Å; C52-H52…F3, 2.46 Å).

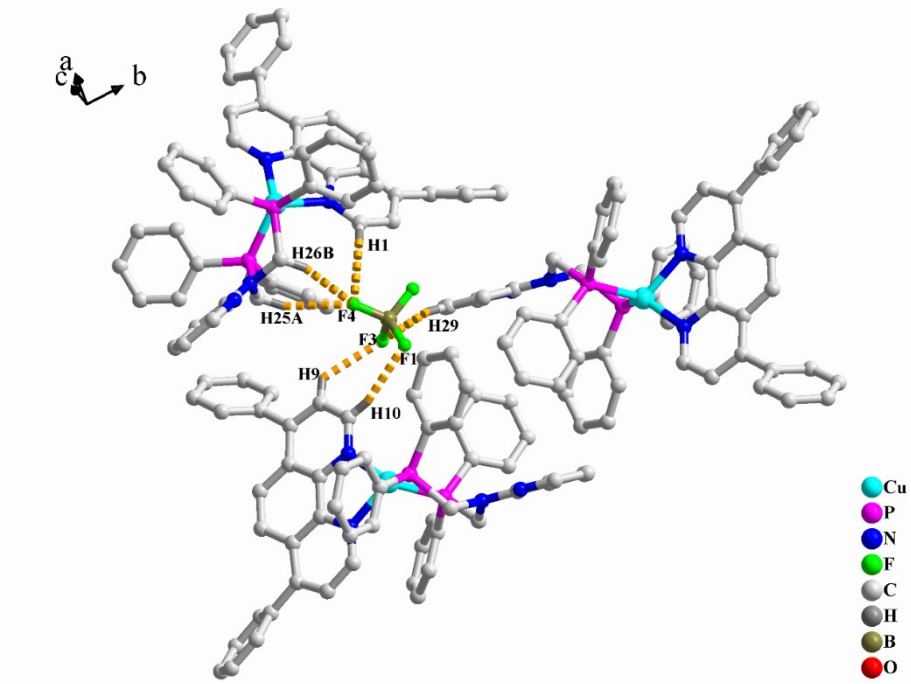

Fig. S24 Hydrogen bonds in **2** (C1-H1…F4, 2.55 Å; C9-H9…F3, 2.46 Å; C10-H10…F1, 2.41 Å; C25-H25A…F4, 2.50 Å; C26-H26B…F4, 2.37 Å; C29-H29…F3, 2.39 Å).

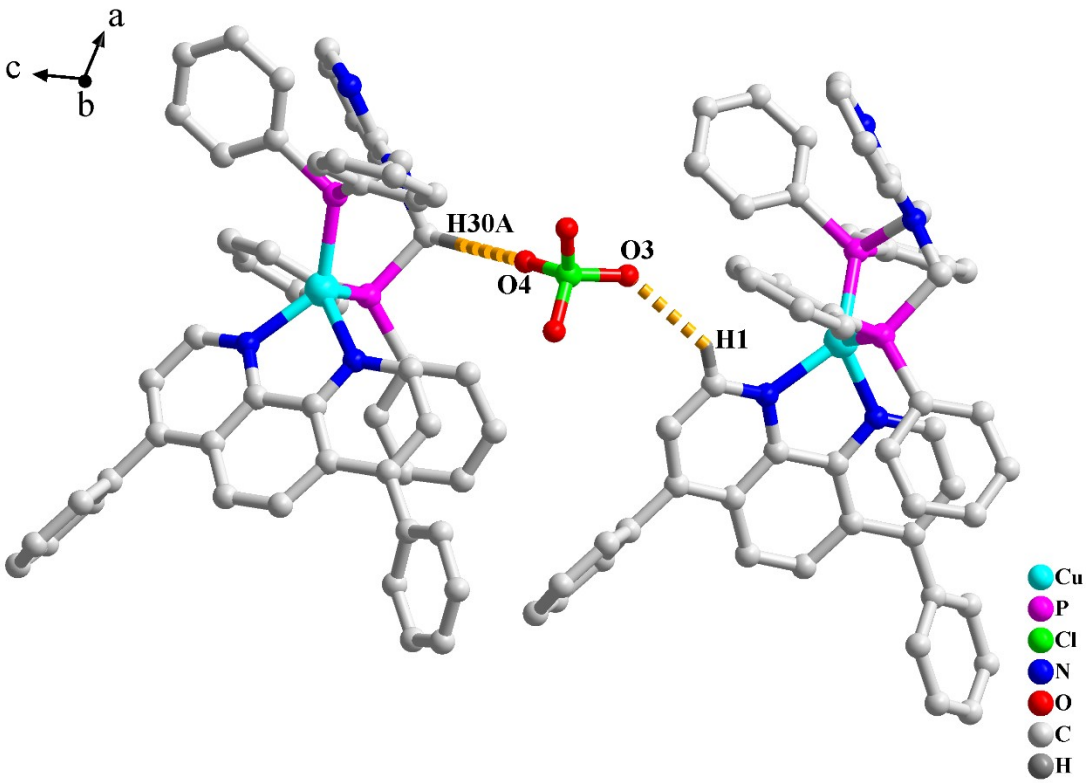

Fig. S25 Hydrogen bonds in **3** (C1-H1…O3, 2.36 Å; C30-H30A…O4, 2.44 Å).

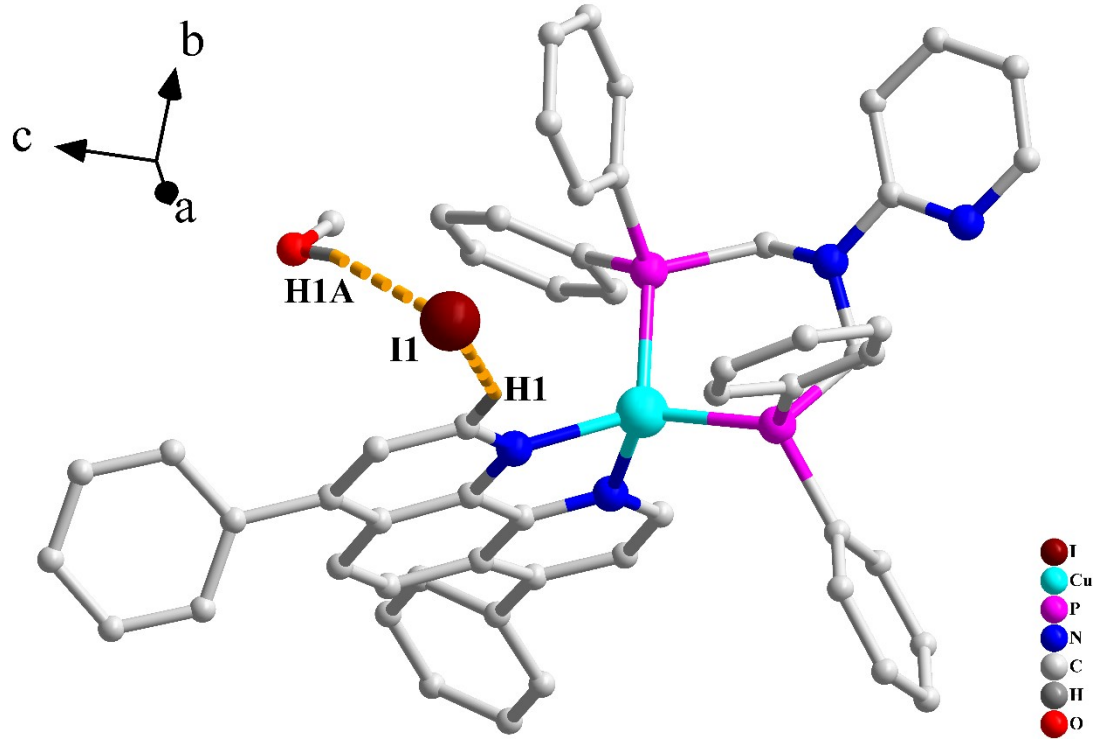

Fig. S26 Hydrogen bonds in **4** (O1-H1A…I1, 2.82 Å; C1-H1…I1, 3.06 Å).

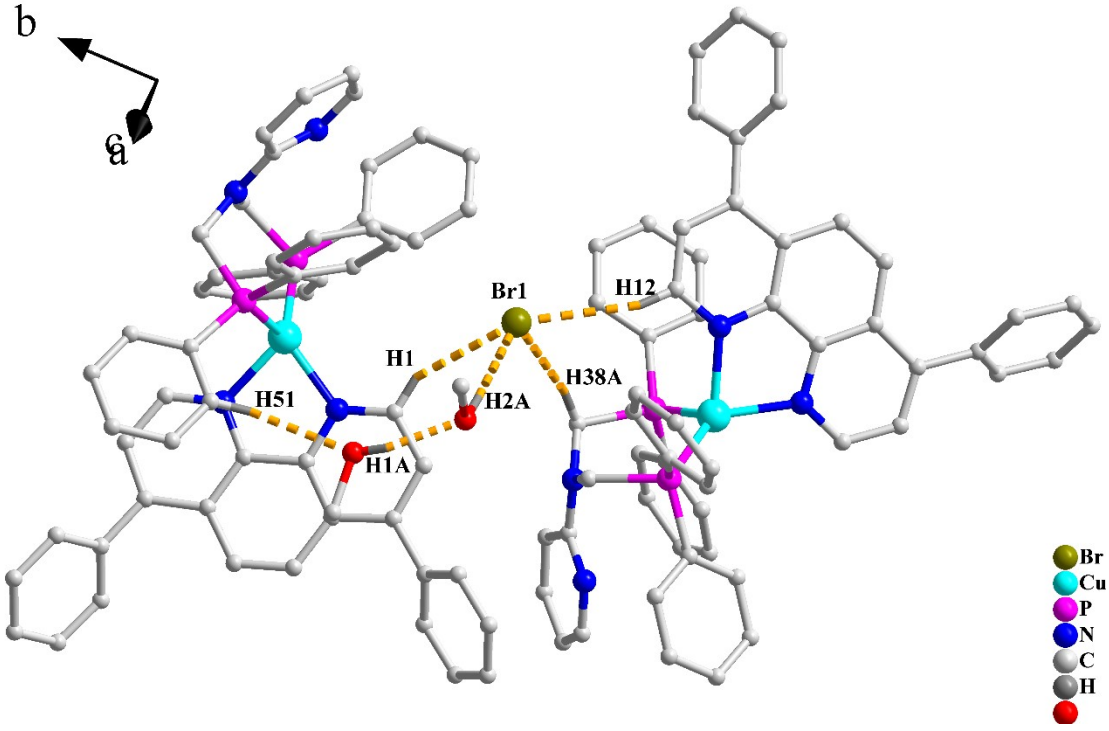

Fig. S27 Hydrogen bonds in **5** (O1-H1A…O2, 1.90 Å; O2-H2A…Br1, 2.48 Å; C1-H1…Br1, 2.86 Å; C12-H12…Br1, 2.85 Å; C38-H38…Br1, 2.86 Å; C51-H51…O1, 2.56 Å;).

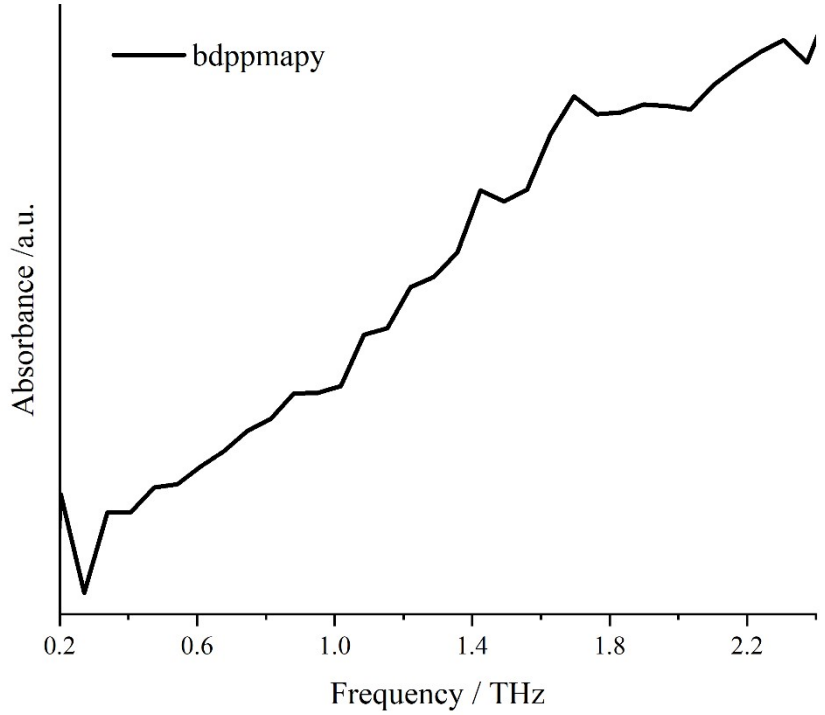

Fig. S28 Terahertz time-domain spectroscopy (THz-TDS) of bdppmapy.

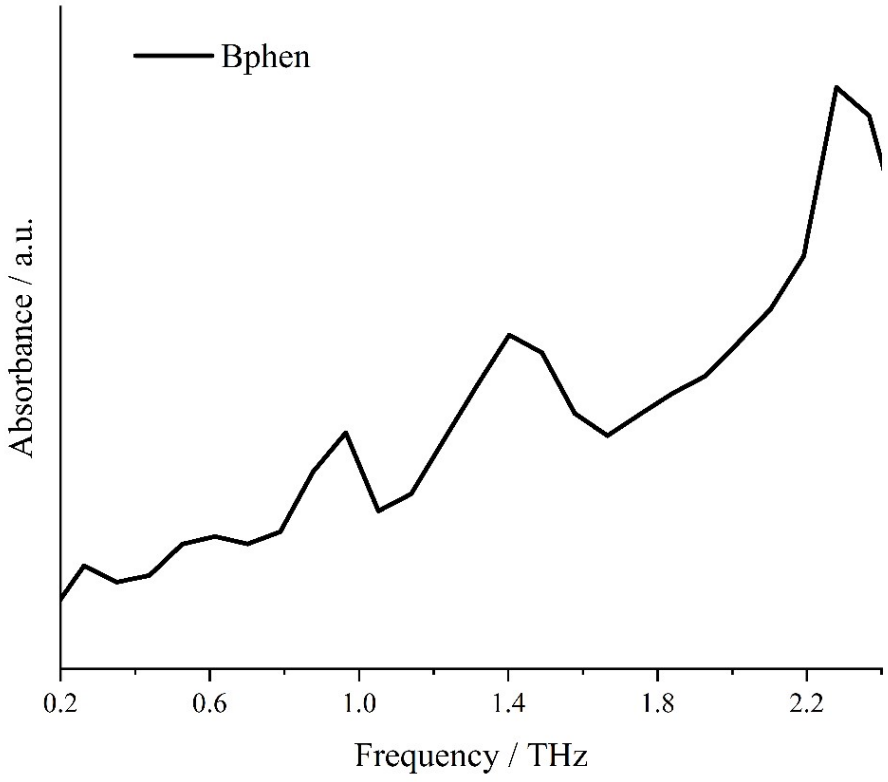

Fig. S29 Terahertz time-domain spectroscopy (THz-TDS) of Bphen.

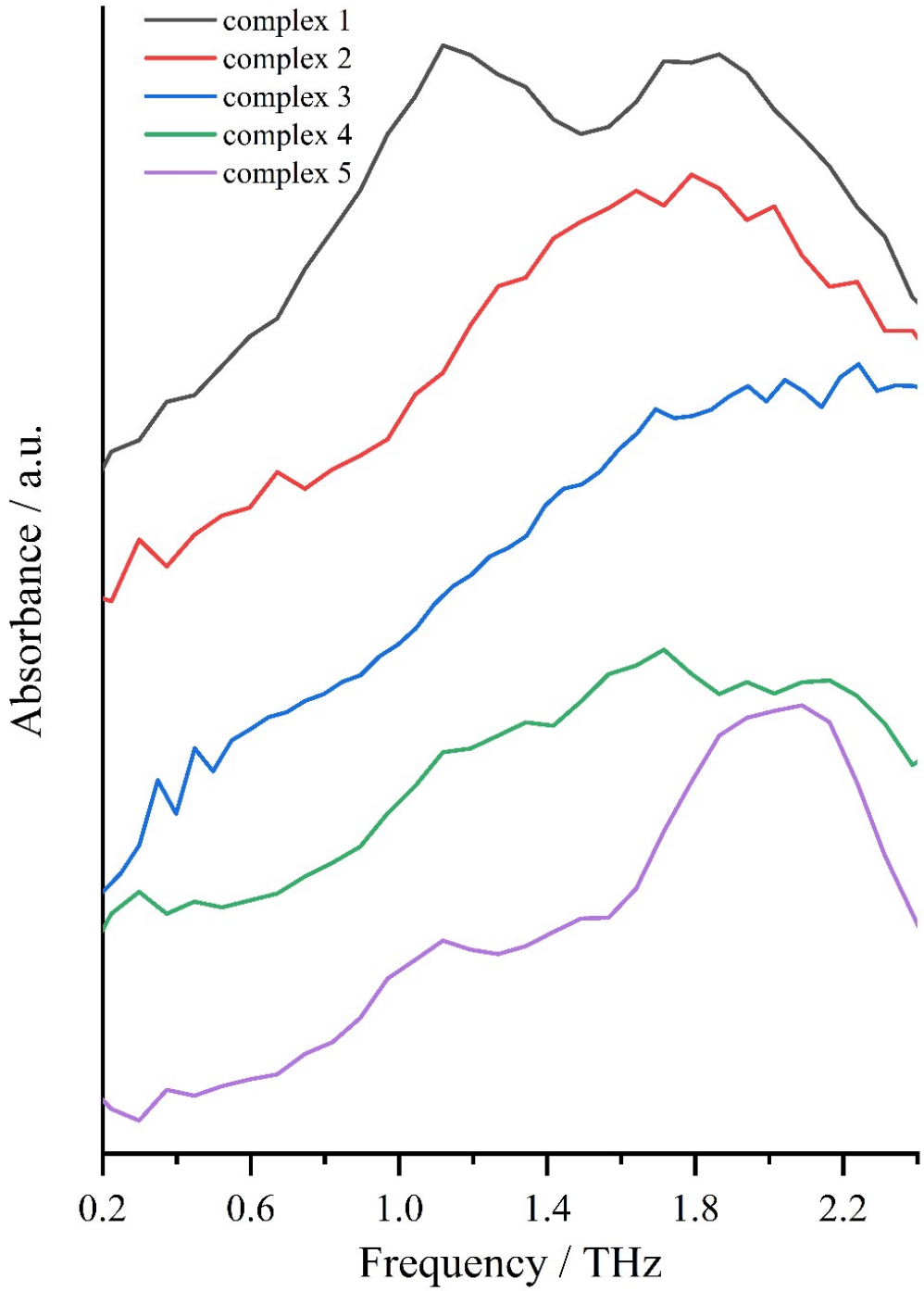

Fig. S30 Terahertz time-domain spectroscopy (THz-TDS) of complexes 1-5.

Table. S1 Selected bond lengths (Å) and angles (°) for complexes **1**-**5**.

Complex **1**			
Cu(1)-I(1)	2.6814(7)	N(1)-Cu(1)-I(1)	80.80(7)
Cu(1)-N(1)	2.0700(33)	N(1)-Cu(1)-P(1)	124.22(5)
Cu(1)-P(1)	2.2838(11)	N(1)-Cu(1)-P(2)	105.46(5)
Cu(1)-P(2)	2.2912(9)	I(1)-Cu(1)-P(1)	127.14(5)
		I(1)-Cu(1)-P(2)	111.74(5)
		P(1)-Cu(1)-P(2)	104.99(2)
Complex **2**			
Cu(1)-N(1)	2.0647(18)	N(1)-Cu(1)-N(2)	80.745(66)
Cu(1)-N(2)	2.0574(17)	N(1)-Cu(1)-P(1)	108.245(53)
Cu(1)-P(1)	2.2580(7)	N(1)-Cu(1)-P(2)	116.361(49)
Cu(1)-P(2)	2.2244(6)	N(2)-Cu(1)-P(1)	116.290(53)
		N(2)-Cu(1)-P(2)	132.189(15)
		P(1)-Cu(1)-P(2)	100.759(24)
Complex **3**			
Cu(1)-N(1)	2.048(3)	N(1)-Cu(1)-N(2)	80.78(10)
Cu(1)-N(2)	2.051(3)	N(1)-Cu(1)-P(1)	108.21(7)
Cu(1)-P(1)	2.2503(9)	N(1)-Cu(1)-P(2)	132.19(8)
Cu(1)-P(2)	2.2196(9)	N(2)-Cu(1)-P(1)	104.83(7)
		N(2)-Cu(1)-P(2)	121.45(8)
		P(1)-Cu(1)-P(2)	105.59(3)
Complex **4**			
Cu(1)-N(1)	2.055(2)	N(1)-Cu(1)-N(2)	80.88(9)
Cu(1)-N(2)	2.047(2)	N(1)-Cu(1)-P(1)	118.14(7)
Cu(1)-P(1)	2.2525(8)	N(1)-Cu(1)-P(2)	105.78(7)
Cu(1)-P(2)	2.2109(8)	N(2)-Cu(1)-P(1)	135.23(7)
		N(2)-Cu(1)-P(2)	112.78(7)
		P(1)-Cu(1)-P(2)	100.86(3)
Complex **5**			
Cu(1)-N(1)	2.066(5)	N(1)-Cu(1)-N(2)	80.84(19)
Cu(1)-N(2)	2.033(5)	N(1)-Cu(1)-P(1)	99.03(13)
Cu(1)-P(1)	2.2575(15)	N(1)-Cu(1)-P(2)	121.12(14)
Cu(1)-P(2)	2.2061(15)	N(2)-Cu(1)-P(1)	116.48(14)
		N(2)-Cu(1)-P(2)	129.55(14)
		P(1)-Cu(1)-P(2)	104.78(6)

Table. S2 Intermolecular C-H…π interactions for complex **1**.

C-H…Cg(*i*)	H…Cg distance / Å	C-H…Cg angel/(°)	C…Cg distance / Å
C20-H20→Cg(3)^{i}	2.91	116	3.414

Cg(3)=N1-C6-C7-C10-C11-C12

Symmetric codes: ^{i} 0.5-x, 2-y, 1-z

Table. S3 Intermolecular C-H…π interactions for complex **2**.

C-H…Cg(*i*)	H…Cg distance / Å	C-H…Cg angel/(°)	C…Cg distance / Å
C14-H14→Cg(4)^{i}	2.84	117	3.37
C36-H36→Cg(12)^{ii}	2.92	136	3.65
C56-H56C→Cg(4)^{iii}	2.41	166	3.35

Cg(4)=N2-C6-C7-C8-C9-C10

Cg(12)=C50-C51-C52-C53-C54-C55

Symmetric codes: ^{i} 2-x, -y, 2-z; ^{ii} -0.5+x, 0.5-y, 0.5+z; ^{iii} x, y, z

Table. S4 Intermolecular C-H…π interactions for complex **3**.

C-H…Cg(*i*)	H…Cg distance / Å	C-H…Cg angel/(°)	C…Cg distance / Å
C17-H17→Cg(8)^{i}	2.86	127	3.50
C18-H18→Cg(9)^{ii}	2.85	171	3.77
C20-H20→Cg(3)^{iii}	2.77	118	3.30
C33-H33→Cg(10)^{ii}	2.86	148	3.69

Cg(3) = N1-C1-C2-C3-C4-C5

Cg(8) = C19-C20-C21-C22-C23-C24

Cg(9) = C31-C32-C33-C34-C35-C36

Cg(10)=C37-C38-C39-C40-C41-C41

Symmetric codes: ^{i} x, 0.5-y, 0.5+z; ^{ii} 1-x, 1-y, -z; ^{iii} 1-x, -y, -z

Table. S5 Intermolecular C-H…π interactions for complex **4**.

C-H…Cg(*i*)	H…Cg distance / Å	C-H…Cg angel/(°)	C…Cg distance / Å
C8-H8→Cg(12)^{i}	2.94	138	3.688
C20-H20→Cg(3)^{i}	2.71	137	3.455
C33-H33→Cg(12)^{ii}	2.89	133	3.584

Cg(3) = N1-C1-C2-C3-C4-C5

Cg(12) = C50-C51-C52-C53-C54-C55

Symmetric codes: ^{i} 1-x, 1-y, 1-z; ^{ii} -0.5+x, 1.5-y, 0.5+z

Table. S6 Intermolecular C-H…π interactions for complex **5**.

C-H…Cg(*i*)	H…Cg distance / Å	C-H…Cg angel/(°)	C…Cg distance / Å
C23-H23→Cg(12)^{i}	2.97	153	3.823
C28-H28→Cg(7)^{ii}	2.76	149	3.584
C40-H40→Cg(7)^{iii}	3.00	154	3.854
C52-H52→Cg(9)^{iv}	2.91	141	3.682

Cg(7) = C13-C14-C15-C16-C17-C18

Cg(9) = C25-C26-C27-C28-C29-C30

Cg(12) = C50-C51-C52-C53-C54-C55

Symmetric codes: [i] 0.5-x, -0.5+y, 1.5-z; [ii] 1+x, y, z; [iii] 0.5+x, 1.5-y, 0.5+z; [iv] -1+x, y, z

Table. S7 Intermolecular π…π interactions for complex **2**.

Cg…Cg(*i*)	Cg…Cg distance / Å	Alpha
Cg(10)…Cg(10)[i]	3.89	0

Cg(10) = C38-C39-C40-C41-C42-C43

Symmetric codes: [i] 2-x, 1-y, 2-z

Table. S8 Intermolecular π…π interactions for complex **3**.

Cg…Cg(*i*)	Cg…Cg distance / Å	Alpha
Cg(5)…Cg(5)[i]	3.81	0

Cg(5) = N4-C25-C26-C27-C28-C29

Symmetric codes: [i] 2-x, 1-y, -z

Table. S9 Fluorescence data for ligands Bphen and bdppmapy.

ligands	λ_{ex} / nm	λ_{em} / nm
Bphen	365	405
bdppmapy	380	433

Table. S10 Energy, oscillator strength and major contribution of the calculated transitions for complex **3.**

Excited state	Energy	Oscillator strength	Contribution %	
3 absorption	2.6213 eV 472.98 nm	0.1760	HOMO-2→LUMO	3.62
			HOMO→LUMO	**92.89**
3 absorption	3.9137 eV 316.80 nm	0.2378	HOMO-12→LUMO+1	2.17
			HOMO-5→LUMO+1	**67.30**
			HOMO-4→LUMO	13.92
			HOMO→LUMO+3	3.20
3 absorption	4.7432 eV 261.39 nm	0.1500	HOMO-20→LUMO	6.63
			HOMO-19→LUMO+1	3.24
			HOMO-18→LUMO+1	3.83
			HOMO-5→LUMO+2	5.00
			HOMO-4→LUMO+5	3.15
			HOMO-3→LUMO+3	8.78
			HOMO-2→LUMO+4	3.29
			HOMO-2→LUMO+5	8.50
			HOMO-2→LUMO+6	**31.29**
			HOMO-1→LUMO+10	2.60
3 emission	2.7022 eV 458.83 nm	0.1496	**LUMO→HOMO-2**	**87.16**